Dietary supplementation of salidroside alleviates liver lipid metabolism disorder and inflammatory response to promote hepatocyte regeneration via PI3K/AKT/Gsk3-β pathway

Zhifu Cui,[*,#] Ningning Jin,[*] Felix Kwame Amevor ⓘ,[*] Gang Shu,[†] Xiaxia Du,[*] Xincheng Kang,[*] Zifan Ning,[*] Xun Deng,[*] Yaofu Tian,[*] Qing Zhu,[*] Yan Wang,[*] Diyan Li,[*] Yao Zhang,[*] Xiaoqi Wang,[‡] Xue Han,[§] Jing Feng,[¶] and Xiaoling Zhao[*,1]

[*]Farm Animal Genetic Resources Exploration and Innovation Key Laboratory of Sichuan Province, Sichuan Agricultural University, Chengdu 611130, P. R. China; [#]College of Animal Science and Technology, Southwest University, Chongqing, P. R. China; [†]Department of Pharmacy, College of Veterinary Medicine, Sichuan Agricultural University, Chengdu, Sichuan Province, P. R. China; [‡]Agriculture and Animal Husbandry Comprehensive Service Center of Razi County, Tibet Autonomous Region, P. R. China; [§]Guizhou Institute of Animal Husbandry and Veterinary Medicine, Guizhou province, P. R. China; and [¶]Institute of Animal Husbandry and Veterinary Medicine, College of Agriculture and Animal Husbandry, Tibet Autonomous Region, P. R. China

ABSTRACT Fatty liver hemorrhagic syndrome (**FLHS**) is a chronic hepatic disease which occurs when there is a disorder in lipid metabolism. FLHS is often observed in caged laying hens and characterized by a decrease in egg production and dramatic increase of mortality. Salidroside (**SDS**) is an herbal drug which has shown numerous pharmacological activities, such as protecting mitochondrial function, attenuating cell apoptosis and inflammation, and promoting antioxidant defense system. We aimed to determine the therapeutic effects of SDS on FLHS in laying hens and investigate the underlying mechanisms through which SDS operates these functions. We constructed oleic acid (**OA**)-induced fatty liver model in vitro and high-fat diet-induced FLHS of laying hens in vivo. The results indicated that SDS inhibited OA-induced lipid accumulation in chicken primary hepatocytes, increased hepatocyte activity, elevated the mRNA expression of proliferation related genes PCNA, CDK2, and cyclinD1 and increased the protein levels of PCNA and CDK2 ($P < 0.05$), as well as decreased the cleavage levels of Caspase-9, Caspase-8, and Caspase-3 and apoptosis in hepatocytes ($P < 0.05$). Moreover, SDS promoted the phosphorylation levels of PDK1, AKT, and Gsk3-β, while inhibited the PI3K inhibitor ($P < 0.05$). Additionally, we found that high-fat diet-induced FLHS hens had heavier body weight, liver weight, and abdominal fat weight, and severe steatosis in histology, compared with the control group (**Con**). However, hens fed with SDS maintained lighter body weight, liver weight, and abdominal fat weight, as well as normal liver without hepatic steatosis. In addition, high-fat diet-induced FLHS hens had high levels of serum total cholesterol (**TC**), triglyceride (**TG**), alanine transaminase (**ALT**), and aspartate aminotransferase (**AST**) compared to the Con group, however, in the Model+SDS group, the levels of TC, TG, ALT, and AST decreased significantly, whereas the level of superoxide dismutase (**SOD**) increased significantly ($P < 0.05$). We also found that SDS significantly decreased the mRNA expression abundance of PPARγ, SCD, and FAS in the liver, as well as increased levels of PPARα and MTTP, and decreased the mRNA expression of TNF-α, IL-1β, IL-6, and IL-8 in the Model+SDS group ($P < 0.05$). In summary, this study showed that 0.3 mg/mL SDS attenuated ROS generation, inhibited lipid accumulation and hepatocyte apoptosis, and promoted hepatocyte proliferation by targeting the PI3K/AKT/Gsk3-β pathway in OA-induced fatty liver model in vitro, and 20 mg/kg SDS alleviated high-fat-diet-induced hepatic steatosis, oxidative stress, and inflammatory response in laying hens in vivo.

Key words: layer, fatty liver hemorrhagic syndrome, salidroside, inflammatory response, hepatocyte proliferation

INTRODUCTION

In poultry, the liver has strong lipid synthesis ability but poor lipid storage capacity. Excessive storage of lipid substances in the liver results in a series of pathological

disorders in aging chickens, in which the most representative disease is fatty liver-hemorrhagic syndrome (**FLHS**) of laying hens, which seriously decreases egg production (Wolford and Polin, 1972; Jensen et al., 1976; Squires and Leeson, 1988; Neuschwander-Tetri, 2007). Further deterioration of fatty liver may lead to steatohepatitis, liver fibrosis, and even cirrhosis (Koek et al., 2011), having sudden death of individuals in the layer flocks (Butler, 1976; Shini et al., 2019).

Studies indicated that high fat diets led to fat transport obstruction in chicken liver, disrupted the dynamic balance of fat metabolism in hepatocytes, adipocytes, and blood. Excessive deposition of lipids are mainly composed of neutral fat in hepatocytes (Egnatchik et al., 2014), which is an important pathological feature of non-alcoholic fatty liver disease (**NAFLD**) (Koo, 2013; Wang et al., 2014; Reccia et al., 2017). Excessive lipid accumulation and estrogen secretion depressed the mitochondrial function in hepatocytes, and produced harmful reactive oxygen species (**ROS**) which damaged hepatocytes, and further reduced the activity of antioxidant enzymes in organisms by inhibiting gene transcription, thus causing damage to the antioxidant system of animals (Mantena et al., 2008).

Plant extracts were reported to improve liver steatosis (Feng et al., 2017; Huang et al., 2018; Wang et al., 2020). *Rhodiola rosea* L. radix (**RRL**) known as plateau ginseng is a rare medicinal herb that grows in cold high-altitude areas. In Ming Dynasty, China (500 yr ago) RRL has used as a tonic to treat diseases, eliminate fatigue and resist cold. Modern pharmacological studies have confirmed that RRL extract has antiaging, antitumor, antihypoxia, antifatigue, and antioxidation functions (Yu et al., 2007; Dhar et al., 2013; Lu et al., 2013; Yuan et al., 2013; Lv et al., 2016; Yang et al., 2016).

Salidroside (**SDS**) is the main pharmacological component of RRL. SDS can scavenge free radicals, decrease oxidative stress, enhance immunity, and prevent aging in animals (Yu et al., 2007; Dhar et al., 2013; Lu et al., 2013; Yuan et al., 2013; Lv et al., 2016; Yang et al., 2016). Meanwhile, SDS has no genetic toxicity or mutagenesis (Zhu et al., 2010). Mao et al. (2010) induced the aging model with D-galactose in mice, and found that SDS could inhibit the formation of advanced glycation end products in vivo, which increased the production of lymphocyte mitosis and interleukin-2 (**IL-2**), and had an antiaging effect. Lu et al. (2013) studied the effects of SDS on the number of helper T cells and the delayed type hypersensitivity response in aged rats, and found that SDS stimulated the body's humoral and cellular immune responses. Zhang et al. (2007) found that SDS inhibited H_2O_2-induced cell viability loss, reduced cell apoptosis rate, inhibited mitochondrial membrane potential decline, and increased intracellular Ca^{2+} concentration, therefore, could be used for treating and preventing neurodegenerative diseases (Zhang et al., 2007). Guan et al. (2012) demonstrated SDS resisted lipopolysaccharide (**LPS**)-induced acute pneumonia in a mouse model (Guan et al., 2012). Li et al. (2013) reported that SDS prevented mouse mastitis induced by LPS, reduced

the activity of myeloperoxidase and the concentrations of TNF-α, IL-1β, and IL-6 in breast muscle tissue, inhibited the inflammatory cell infiltration, and produced anti-inflammatory effects.

In addition, SDS was reported to exert antioxidant protective effect against LPS-induced liver damage in mice, as well as inhibited hypoxia-inducible factor-1α expression (Wu et al., 2009), and protected against acetaminophen-induced hepatotoxicity by preventing or mitigating intracellular glutathione depletion and oxidative damage (Wu et al., 2008), and inhibited chronic hepatitis C virus by inhibiting serine protease activity (Zuo et al., 2007). Recent studies indicated that SDS alleviated hypoxia-induced liver injury and inhibited cell apoptosis via the IRE1α/JNK pathway (Xiong et al., 2020), alleviated carbon tetrachloride-induced liver damage in mice by activating mitochondria to resist oxidative stress (Lin et al., 2019), inhibited apoptosis and autophagy in a Concanavalin A-induced liver injury model (Feng et al., 2018). Moreover, SDS also protected oxidative stress induced by diabetes mellitus, effectively reduced serum TC and TG levels (Li et al., 2011), alleviated liver steatosis in type 2 diabetic mice (Zhang et al., 2016b), and reduced obesity and liver lipid deposition induced by a high-fat diet by inhibiting oxidative stress and activation of inflammatory cytokines in the liver (Zheng et al., 2018).

Generally, SDS could protect the liver and also use in treating liver diseases in mammals. Among these studies, Oleic acid (**OA**) (Weijler et al., 2018; Espe et al., 2019; Li et al., 2020) is usually used to induce fatty liver models in vitro. Therefore, in this study, we hypothesize that SDS may have positive effect on relieving the fatty liver in laying hens. In this present study, we used OA, dietary energy, and protein structure recombination (Maurice and Jensen, 1978; Rozenboim et al., 2016; Yang et al., 2017; Zhuang et al., 2019) to establish chicken fatty liver models in vitro and in vivo to explore the effects of SDS on lipid metabolism, proliferation, apoptosis, and mitochondrial function of fatty liver in chickens, and to investigate the underlying mechanisms through which SDS operates these functions.

MATERIALS AND METHODS

Purity Determination of SDS

The SDS was purchased from Nanjing Herb-Source Biotechnology Co. Ltd (Nanjing, China). Its purity and structure were examined via High Performance Liquid Chromatography (**HPLC**; Agilent Technologies Inc., CA), Nuclear Magnetic Resonance Spectrometer (**NMR**; Avance III HD 400, Bruker, Switzerland), and Mass Spectrometry (**MS**; Thermo Fisher Scientific, San Jose, CA).

Animals

A total of 360 (35-wk-old) Rohman layers were raised at the Poultry Breeding Unit, Sichuan Agricultural University (Ya'an, China). Each bird was raised in a single

cage (size: 500 mm × 400 mm × 370 mm), and water was provided ad libitum. All animal experiments were approved by the Institutional Animal Care and Use Committee of Sichuan Agricultural University (Certification No. SYXK2019-187). All experiments were conducted in accordance with the Laboratory Animal Welfare and Ethics guidelines of Sichuan Agricultural University.

Cell Culture and Treatment

A total of 36 birds were used for the in vitro experiments. Primary hepatocytes were isolated from 2 Rohman layers each time according to the methods described previously (Zhou et al., 2012; Qi et al., 2018). The hepatocytes were resuspended in William's medium E (Sigma, Shanghai, China) and plated into 6-well plates (2×10^6 cells/well) after cell counting. The hepatocytes were cultured in a cell culture incubator at a constant temperature of 37°C, 5% CO_2, and 95% air saturated humidity. After 24 h, the hepatocytes were cultured with 0.6 mM OA (Li et al., 2020) for 12, 24, 36, and 48 h and treated with/without SDS (0.1, 0.2, 0.3, 0.4 mg/mL). All hepatocytes were collected for further experiments.

RNA Extraction and Quantitative Real Time PCR

Total RNA was extracted from all the samples (in vitro experiments hepatocytes and in vivo experiment liver tissues) according to the instructions of the Trizol reagent (Molecular Research Center, Cincinnati, OH). The RNA concentration and purity were estimated by determining the A260/A280 absorbance ratio, and the 18 S and 28 S bands in a 1% agarose gel. Reverse transcription and qRT-PCR were performed as previously described (Cui et al., 2020a). *GAPDH* and β-actin were used as endogenous controls to normalize gene expression using the $2^{-\Delta\Delta Ct}$ method (Livak and Schmittgen, 2001). Gene-specific primers designed with software Primer Premier 5.0 according to the coding sequences of target genes are summarized in Table 1.

Protein Extraction and Western Blot Analysis

Protein isolation was performed from the hepatocyte using protein extraction kit (BestBio Biotech Co. Ltd., Shanghai, China), and the BCA protein assay kit (BestBio) was used to determine the concentration of protein samples. Western blotting was performed with following the method described previously (Cui et al., 2020b) with the following primary antibodies: anti-PPARα (1:2,000, ab233078, Abcam, Cambridge, UK), anti-PCNA (1:1,000, A0264, ABclonal Technology, Wuhan, China), anti-CDK2 (1:500, 120395, Zen-Bio, Chengdu, China), anti-caspase-3 (1:5,000, ab214430, Abcam) and caspase-8 (1:1,000, ab227430, Abcam), and caspase-9 (1:1,000,

bs-20773R, Bioss, Beijing, China), anti-PDK1 [1:1,000, #3062, Cell Signaling Technology (CST), Boston, United States], anti-p-PDK1 (1:1,000, #3061, CST), anti-AKT (1:1,000, #9272, CST) and p-AKT (1:1,000, #9271, CST), and anti-Gsk3-β (1:1,000, A2081, ABclonal) and p-Gsk3-β (1:1,000, AP0261, ABclonal). Secondary antibodies: goat anti-mouse (1:5,000, 511103, Zen-Bio) and goat anti-rabbit (1:5,000, 511203, Zen-Bio). β-Tubulin (1:1,000, 250063, Zen-Bio) was used as a reference.

Staining for Liver Tissue

Six chickens (6) from each group were randomly selected and euthanized, and their liver tissues were collected. The left lobe liver was selected and the vernier caliper was used to ensure the samples were collected from the same tissue areas. Six (6) liver tissue samples were obtained from each group, however, three (3) liver samples (μm/g) were fixed with 4 % paraformaldehyde for 24 h and dehydrated with different concentrations of alcohol. Thereafter, the tissue was embedded in paraffin, cut into thin slices (3−5 μm) and placed on a slide. After hematoxylin and eosin (**HE**) staining, the HE sections were sealed with neutral resin. Then, the remaining three (3) fresh liver samples were cut in the size of 24 mm × 24 mm × 2 mm, frozen and then were placed on a tissue bearer dripping with an OTC embedding agent. Slices (thickness 10 μm) were obtained with the slicing machine (Leica CM1520, Germany) and affixed to the anti-slip slide. After staining with oil red O staining solution for 15 min, the slices were sealed with a neutral resin. Six sections (3 HE sections and 3 oil red O staining sections) per treatment were used for the data collection. All sections were viewed under a microscope (DP80Digital, Olympus, Tokyo, Japan) and ten fields were randomly selected for statistical analysis.

Cell Counting Kit−8 and 5−ethynyl−2−deoxyuridine Assay

The Cell Counting Kit−8 (**CCK-8 Kit**) (Meilun-Bio, Dalian, China) was used to test hepatocyte activity and choose the optimum concentration and treatment time of SDS in the OA-induced fatty liver model of primary hepatocytes. Ten μL of CCK−8 reagent was added to each well and incubated in a cell culture incubator for 2 h after being treated with SDS for 12, 24, 36, and 48 h. A microplate reader (Varioskan LUX, Thermo Fisher) was used to determine the optical density (**OD**) of each sample at 450 nm. The proliferation state of hepatocytes was determined using a Cell−Light™ EdU kit (RiboBio, Guangzhou, China) according to the manufacturer's instructions. A fluorescent microscope was used to calculate the number of 5−ethynyl−2−deoxyuridine (**EdU**)-positive cells.

Table 1. Primers used for qRT-PCR.

Gene	Sequence (5'-3')	Product Length (bp)	Annealing Temperature (℃)	Accession Number
PPARα	F: AGGCCAAGTTGAAAGCAGAA R: TTTCCCTGCAAGGATGACTC	155	60	NM_001001464.1
PPARγ	F: TGACAGGAAAGACGACAGACA R: CTCCACAGAGCGAAACTGAC	164	59	NM_001001460.1
ACSL1	F: TACCCTGGTGGGTTTTGGTG R: AGGAGAGAGGACCTTCGAGC	144	55	NM_001012578.1
FASN	F: TGCTATGCTTGCCAACAGGA R: ACTGTCCGTGACGAATTGCT	128	59	NM_205155.3
MTTP	F: GTTCTGAAGGACATGCGTGC R: GATGTCTAGGCCGTACGTGG	120	58	NM_001109784.2
FADS1	F: TGGCCTGGATGCTTACCTTC R: AAGGTGGTGCTCGATTTGGA	275	57	XM_421052.5
FADS2	F: GGCCTTCCACATCAATCCCA R: TCCGAAAATCCTCCACCAGC	125	58	NM_001160428.2
PCNA	F: AACACTCAGAGCAGAAGAC R: GCACAGGAGATGACAACA	225	55	NM_204170.2
CDK2	F: GCTCTTCCGTATCTTCCGCA R: ATGCGCTTGTTGGGATCGTA	192	56	NM_001199857.1
CyclinD1	F: TGTCGTTCGAACCCCTCAAG R: TTGCAGTAACTCGTCGGGTC	152	57	NM_205381.1
Caspase-8	F: GGGTGTCTCCGTTCAGGTATC R: CATCTCTCCTTCACCAAGTAAGT	275	57	NM_204592.3
Caspase-9	F: TCCCGGGCTGTTTCAACTT R: CCTCATCTTGCAGCTTGTGC	270	60	XM_424580.6
Caspase-3	F: TGGCCCTCTTGAACTGAAAG R: TCCACTGTCTGCTTCAATACC	106	61	NM_204725.1
IL-1β	F: GGTCAACATCGCCACCTACA R: CATACGAGATGGAAACCAGCAA	86	62	NM_204524.1
IL-6	F: AAATCCCTCCTCGCCAATCT R: CCCTCACGTCTTCTCCATAAA	105	58	NM_204628.1
TNF-α	F: GCCCTTCCTGTAACCAGATG R: ACACGACAGCCAAGTCAACG	71	56	XM_040647307.1
IL-8	F: CAGCGATTGAACTCCGATGC R: CTGCCTTGTCCAGAATTGCC	207	61	NM_205018.1
GAPDH	F: TCCTCCACCTTTGATGCG R: GTGCCTGGCTCACTCCTT	144	59	NM_204305.1
β-actin	F: GAGAAATTGTGCGTGACATCA R: CCTGAACCTCTCATTGCCA	152	60	NM_205518.1

F: Forward primer; R: Reverse primer.

Cell Apoptosis and Reactive Oxygen Species Analysis

Hepatocyte apoptosis was detected using Flow Cytometry (CytoFLEX, Beckman Coulter, CA, USA) and Kaluza 2.1 software. Hepatocytes were washed with PBS and the concentration was adjusted to 1×10^6 cells/mL, and determination was performed as previously described (Cui et al., 2021). DCFH-DA (2, 7-Dichlorofluorescin; Sigma) was added to hepatocytes at a final concentration of 10 μM for 20 min at room temperature, and then the hepatocyte Reactive Oxygen Species (**ROS**) were analyzed using a Shimadzu RF-3501 fluorescence spectrophotometer at an excitation wavelength of 488 nm and an emission wavelength of 525 nm.

PI3K/AKT/Gsk3-β Pathway Analysis

LY294002 (Houston, Texas, United States) was used as a PI3K inhibitor to explore whether SDS exerts its biological function through PI3K/AKT/Gsk3-β. LY294002 was purchased from Selleck Chemicals and pre-incubated with hepatocytes for 2 h. And then, hepatocyte protein was isolated for further western blot analysis.

In Vivo Experiments in Laying Hens

In Trial 1, we aimed to find out the optimal feeding concentration of SDS. Thus, 180 thirty-five-wk-old Rohman layers were randomly divided into 6 groups (30 chickens per group), including the Control (Con) and SDS feeding groups (5, 10, 20, 40, and 80 mg/kg, respectively). The SDS was administered to the chickens orally on daily basis, and the pre-experiment lasted for 4 wk. The blood samples were collected via the wing vein and centrifuged at 3,000 rpm for 10 min at 4°C to obtain the serum. Serum biochemical parameters including total cholesterol (**TC**), Triglyceride (**TG**), alanine aminotransferase (**ALT**), aspartate aminotransferase (AST), and superoxide dismutase (SOD) were measured with the enzyme-linked immunosorbent assay (**ELISA**) kits (Baolai Biotechnology Co., Ltd, Yancheng, China), following the manufacturer's instructions. Moreover, the expression abundances of lipid metabolism-related genes and inflammatory factors were determined using qRT-PCR.

In Trial 2, our purpose was to determine whether SDS can attenuates fatty liver in laying birds. Therefore, 144 (35-wk-old) Rohman layers were allotted into four (4) groups including: Con, Con+SDS, Model, and Model +SDS groups. Based on the Trial 1, optimal feeding dosage of SDS (20 mg/kg) was used to feed the birds for 4

wk in the Con+SDS and Model+SDS groups. The fatty liver model (Model) of the laying hens in vivo was established following the method previously described by (Maurice and Jensen, 1978; Rozenboim et al., 2016; Yang et al., 2017; Zhuang et al., 2019). The diet composition was summarized in Table 2.

Statistical Analysis

The statistical analyses were carried out using SAS 9.3 software (SAS Institute Inc., Cary, NC). The experimental data were first tested by normal distribution, and on this basis, we carried out one-way analysis of variance (**ANOVA**), in which the statistics included the homogeneity test of variance. Percentages were transformed to arc sines of the square roots to fit a normal distribution. Other data were transformed to common logarithms. Transformations were made before ANOVA. All experimental results were presented as mean $\pm$ standard error (SE). Significance level was determined using Duncan's multiple range tests and displayed as $P < 0.05$ (*) and $P < 0.01$ (**).

RESULTS

Purity Determination of SDS

The purity and structure of the SDS ($C_{14}H_{20}O_7$, 300.30, Figure 1A) were detected using HPLC, NMR, and MS. The HPLC analysis results showed that the area reached a peak at a run time of 14.196 min, with a

Table 2. Diet composition for layers.

Ingredient (%)	Control group	Model group
Corn	62.5	62.5
Soybean meal	20.09	20.09
Corn gluten meal	1.5	1.5
DDGS (corn)	3	3
Soybean oil	1	5
CaHPO$_4$	1.04	1.04
Limestone	9	9
NaCl	0.25	0.25
Microecologics	0.05	0.05
Choline	0.1	0.1
Phytase	0.02	0.02
Premix	1.45	1.45
Total	100	104
Nutrient levels		
ME/(MJ/kg)	11.291	11.953
Crude Protein (%)	16.234	15.61
Crude Fat (%)	2.261	2.174
Met (%)	0.234	0.225
Lys (%)	0.769	0
AP (%)	0.306	0.739
TCa (%)	3.567	0.294
TP (%)	0.5	3.43

Premix: Vitamin premix supplied (per kg of diet): Vitamin A, 6000 IU; Vitamin D3, 1,500 IU; Vitamin K3, 4.2 mg; Vitamin B1, 3 mg; Vitamin B2, 10.2 mg; Folic acid, 0.9 mg; Calcium pantothenate, 15 mg; Niacin 45 mg; Vitamin B6, 5.4 mg; Vitamin B12, 24 μg; Biotin 150 μg. Mineral premix provided (per kg of diet): Cu (CuSO$_4$·5H$_2$O), 6.8 mg; Fe (FeSO$_4$· 7H$_2$O), 66 mg; Zn (ZnSO$_4$·7H$_2$O), 83 mg; Mn (MnSO$_4$·H$_2$O), 80 mg; I (KI), 1 mg; Se (Na$_2$SeO$_3$), 0.3 mg.

Abbreviations: AP, Available phosphorus; DDGS, distiller dried grains with solubles; TCa, Total Calcium; TP: Total phosphorus.

peak area rate of 99.81 % (Figure 1B). NMR analysis results showed that the structure complied with the molecular formula of $C_{14}H_{20}O_7$ (Figure 1C). MS analysis showed that the structure complied with the molecular weight of 300.30 Da (Figure 1D).

SDS Treatment With OA-Induced Fatty Liver Model in Primary Hepatocytes

OA (0.6 mM) was used for inducing fatty liver model in the primary hepatocytes. The cells were treated with 0.1, 0.2, 0.3, 0.4 mg/mL SDS for 48 h, respectively (Table 3). According to the OD values of the CCK-8 assay at 12, 24, 36, and 48 h, OA significantly decreased hepatocyte activity compared with the control, whereas SDS significantly increased hepatocyte activity at the concentration of 0.3 mg/mL at 36 h (Figure 2A). The EdU assay revealed a decrease in the number of proliferating cells in response to treatment with OA, whereas the cell proliferation rate significantly increased in the SDS treatment group ($P < 0.05$; Figures 2B and 2C).

SDS Inhibits OA-Induced Lipid Accumulation and Promotes Proliferation in Chicken Primary Hepatocytes

We further explored the effect of SDS on OA-induced fatty liver model. The results showed that the mRNA abundance and protein level of peroxisome proliferator-activated α (**PPARα**) significantly decreased in the OA group, whereas SDS significantly increased the mRNA and protein levels of PPARα ($P < 0.05$; Figures 3A and 3B). The mRNA expression of acyl-CoA synthetase long-chain 1 (**ACSL1**) and microsomal triglyceride transport protein (**MTTP**) were decreased in the OA group. However, SDS increased their mRNA expression levels in group OA+ SDS. The mRNA expression abundances of peroxisome proliferator-activated γ (**PPARγ**), fatty acid synthase (**FASN**), Fatty acid desaturase 1 (**FADS1**), and fatty acid desaturase 2 (**FADS2**) were significantly increased in the OA group while SDS decreased their mRNA expression levels in group OA+ SDS ($P < 0.05$; Figure 3A).

We investigated the effect of SDS on chicken hepatocyte proliferation in an OA-induced fatty liver model. We found that OA resulted in a decrease in the mRNA and protein levels of proliferation related genes (cyclin-dependent kinase 2 [**CDK2**] and proliferating cell nuclear antigen [**PCNA**]), and decreased the mRNA expression of cyclinD1. SDS significantly increased the mRNA expression of PCNA, CDK2, and cyclinD1, as well as the protein expression levels of PCNA and CDK2 ($P < 0.05$); Figures 3C−3E).

SDS Targets the PI3K/AKT/Gsk3-β Pathway

Phosphoinositide 3-kinase (**PI3K**)/AKT-glycogen synthase kinase 3 beta (**Gsk3-β**) is an important anti-popototic signaling pathway that activates a series of

A

OH

OH,,

OH

ÖH
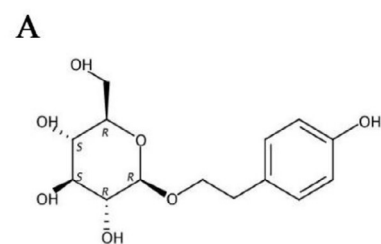
Molecular Formula (M. F.): $C_{14}H_{20}O_7$

Molecular Weight (M. W.): 300.30

B High Performance Liquid Chromatography, HPLC

SAMPLE INFORMATION			
Sample Name:	Salidroside	Acquired By:	System
Vial:	4	Processing Method:	Quality Guarantee System 3
Injection #:	1	Channel Name:	275.0 nm
Injection Volume:	8.00 µL	Proc. Chnl. Descr.:	PDA 275.0 nm
Run Time:	100.0 Minutes		

Auto-Scaled Chromatogram
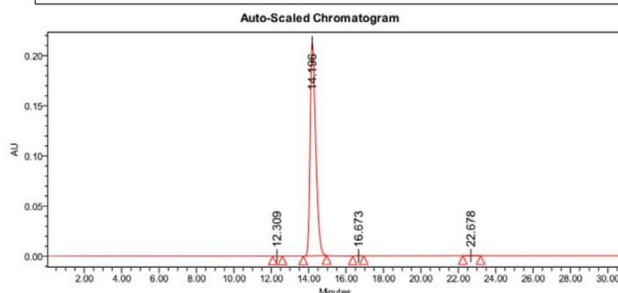
Peak Results			
Name	RT	Area	% Area
1	12.309	1599	0.04
2	14.196	4388053	99.81
3	16.673	2099	0.05
4	22.678	4509	0.10

C Nuclear Magnetic Resonance, NMR

^{1}H-NMR (DMSO)

^{13}C-NMR (DMSO)

D Mass Spectrometry, MS

x10 7 +/-ESI TIC Scan Frag=135.0V CF=0.000 DF=0.000 sd151438.d

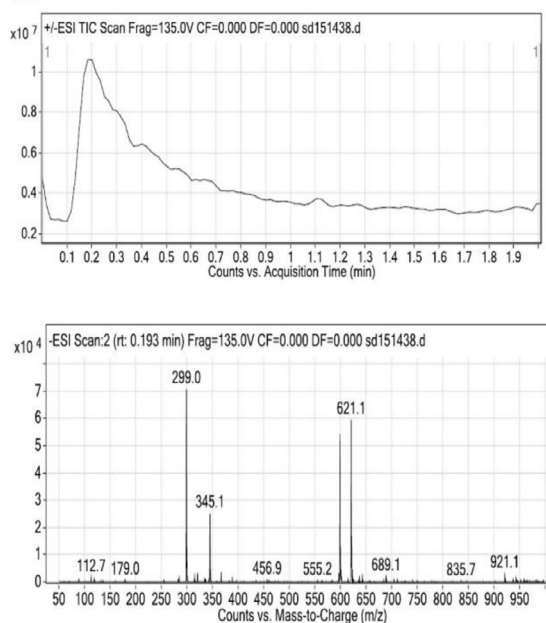x10 4 -ESI Scan:2 (rt: 0.193 min) Frag=135.0V CF=0.000 DF=0.000 sd151438.d
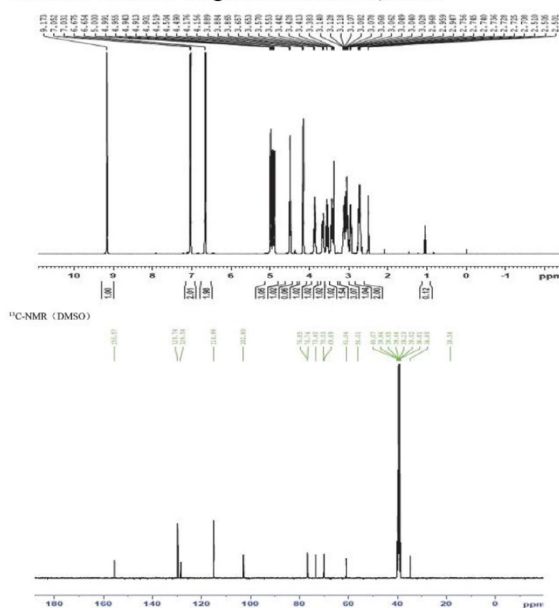
Figure 1. The purity and structure of SDS (A) were detected using HPLC (B), NMR (C), and MS (D).

growth signaling pathways and blocks a series of apoptotic signaling pathways, thus promoting cell survival and proliferation (Pap and Cooper, 1998; Zhang et al., 2016a). In the present study, we attempted to uncover the function and regulation pathways of SDS in an OA-induced fatty liver model. The results showed that protein levels of p-PDK1, p-AKT, and p-Gsk3-β in the OA treated group were lower than those in the NC group ($P < 0.05$), while the SDS (OA+Salidroside) treatment group had higher protein levels than the OA treatment

Table 3. Cell proliferation status detected with CCK-8 kit.

			OD value			
			Salidroside concentration (mg/mL)			
Time point (h)	NC	Oleic acid (OA)	0.1	0.2	0.3	0.4
12	0.359±0.028[a]	0.337±0.017[b]	0.358±0.036[a]	0.378±0.046[a]	0.356±0.017[a]	0.352±0.02[a]
24	0.371±0.036[a]	0.344±0.041[b]	0.377±0.051[a]	0.413±0.017[a]	0.368±0.026[a]	0.383±0.025[a]
36	0.427±0.023[b]	0.344±0.027[c]	0.441±0.031[b]	0.458±0.025[b]	0.517±0.018[a]	0.461±0.023[b]
48	0.461±0.025[a]	0.348±0.018[b]	0.454±0.03[a]	0.452±0.031[a]	0.514±0.036[a]	0.467±0.038[a]

Value were show as mean ± SEM (n = 9)
[a,b,c]Means in the same row marked without a common superscript letter differed significantly ($P < 0.05$). NC: negative control.
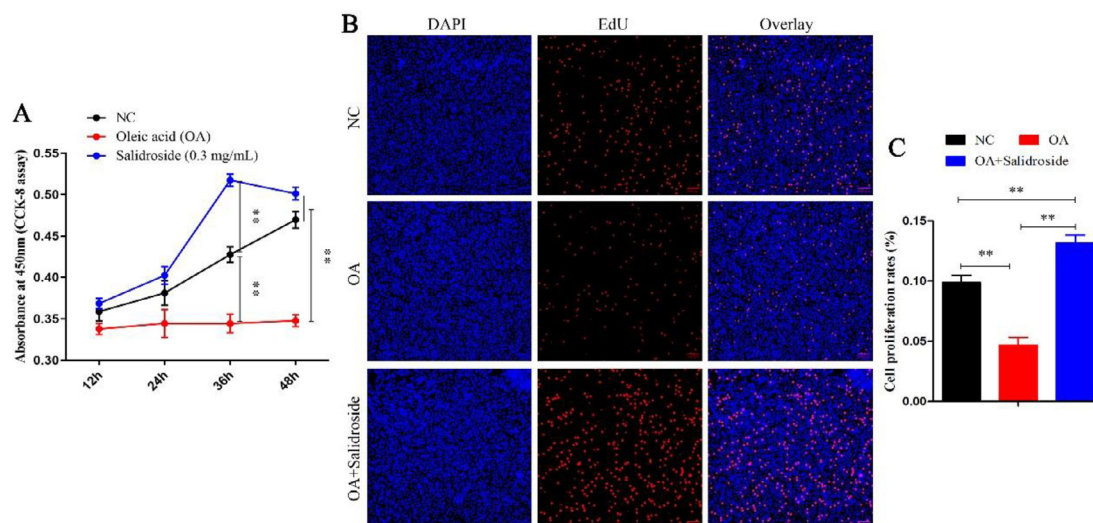
Figure 2. The effect of SDS on viability of primary hepatocytes with OA-induced fatty liver model. (A) The OD values of hepatocytes treated with 0.3 mg/mL Salidroside for 12, 24, 36, and 48 h, respectively. (B, C) EdU staining-positive hepatocytes were detected by EdU kit. Abbreviations: NC, negative control; OA, oleic acid. EdU (red), DAPI (blue); Replications = 3. Bars represent SEM; *$P < 0.05$ and **$P < 0.01$.

group ($P < 0.05$). Moreover, we added LY294002 as a PI3K inhibitor in the SDS treatment group, and found that the protein levels of p-PDK1, p-AKT, and p-Gsk3-β in the PI3K inhibitor (OA+Salidroside +LY294002) treated group were lower than those in the SDS treatment group ($P < 0.05$; Figures 3F and 3G). Generally, SDS inhibits lipid accumulation and promotes hepatocyte proliferation in the OA-induced fatty liver model targeting the PI3K/AKT/Gsk3-β pathway.

SDS Inhibits Hepatocyte Apoptosis in OA-Induced Fatty Liver Model

We further investigated whether SDS influenced hepatocyte apoptosis in OA-induced fatty liver and found that OA significantly increased the mRNA expression of *Caspase-8, Caspase-9*, and *Caspase-3*, and protein expression levels of Caspase-9 and Caspase-3, didn't affect the protein expression of Caspase-8. However, the mRNA expression and cleavage levels of Caspase-9, Caspase-8, and Caspase-3 were significantly decreased in the SDS treatment group ($P < 0.05$) (Figures 4A−4C). Excessive ROS production and mitochondrial dysfunction lead to liver steatosis and hepatocyte apoptosis (Liu et al., 2016; Prieto and Monsalve, 2017). We further examined the effect of SDS on hepatocyte ROS levels in the OA-induced fatty liver model. The results showed that OA led to an increase in the hepatocyte mitochondrial ROS production, whereas SDS significantly decreased the ROS level compared to the NC group ($P < 0.05$; Figures 4D and 4E). An increased number of early and necrotic late apoptosis hepatocytes appeared in the OA-induced fatty liver group, and SDS significantly decreased both early and necrotic late apoptosis in hepatocytes compared with the NC group (Figures 4F and 4G).

SDS Alleviates Hepatic Steatosis and Inflammatory Response of Laying Hens in Vivo

In Trail 1, we found that TC, TG, ALT, and AST levels in the serum of SDS feeding groups were decreased, compared with the Control group (Con). The TC concentration was significantly decreased at the level 10, 20, and 40 mg/kg for SDS, and reached the bottom at the level 20 mg/kg ($P < 0.05$). The AST level was significantly decreased in all SDS concentration groups, compared with the control ($P < 0.05$). There were no significant differences for SOD levels among the groups (Table 4). Moreover, compared to the Con group, the mRNA expression abundance of *PPARα* was significantly increased in SDS 20 mg and 40 mg/kg treatment groups ($P < 0.05$). The mRNA expression of *PPARγ* significantly decreased in the groups 40 and 80 mg/kg SDS ($P < 0.05$). The mRNA expression of *MTTP* was significantly increased in the SDS 5 mg and 20 mg/kg treatment groups ($P < 0.05$). The mRNA expression of *FASN* was significantly decreased at the groups 5, 20, 40 and 80 mg/kg SDS ($P < 0.05$). The mRNA levels of the inflammatory factors *IL-6* and *IL-1β* were significantly decreased in the groups 10, 20, 40, and 80 mg/kg SDS ($P < 0.05$, Table 5).

Based on above results, the optimal feeding concentration of SDS was verified as 20 mg/kg. In Trial 2, we found that the body weight, liver weight, and abdominal fat weight were significantly increased in the Model group, and significantly decreased in the Con + SDS and Model + SDS group, compared with the Con group (Table 6). H & E staining of the liver tissues in the Con group showed that the cytoplasm was lightly stained, and appeared a few small fatty vacuoles. Oil red O staining showed that small lipid droplets appeared in the liver, which indicated mild steatosis. In the Model group, we found a large number of fatty vacuoles, the hepatic cord was disorganized, the sinuses were atretic, and oil
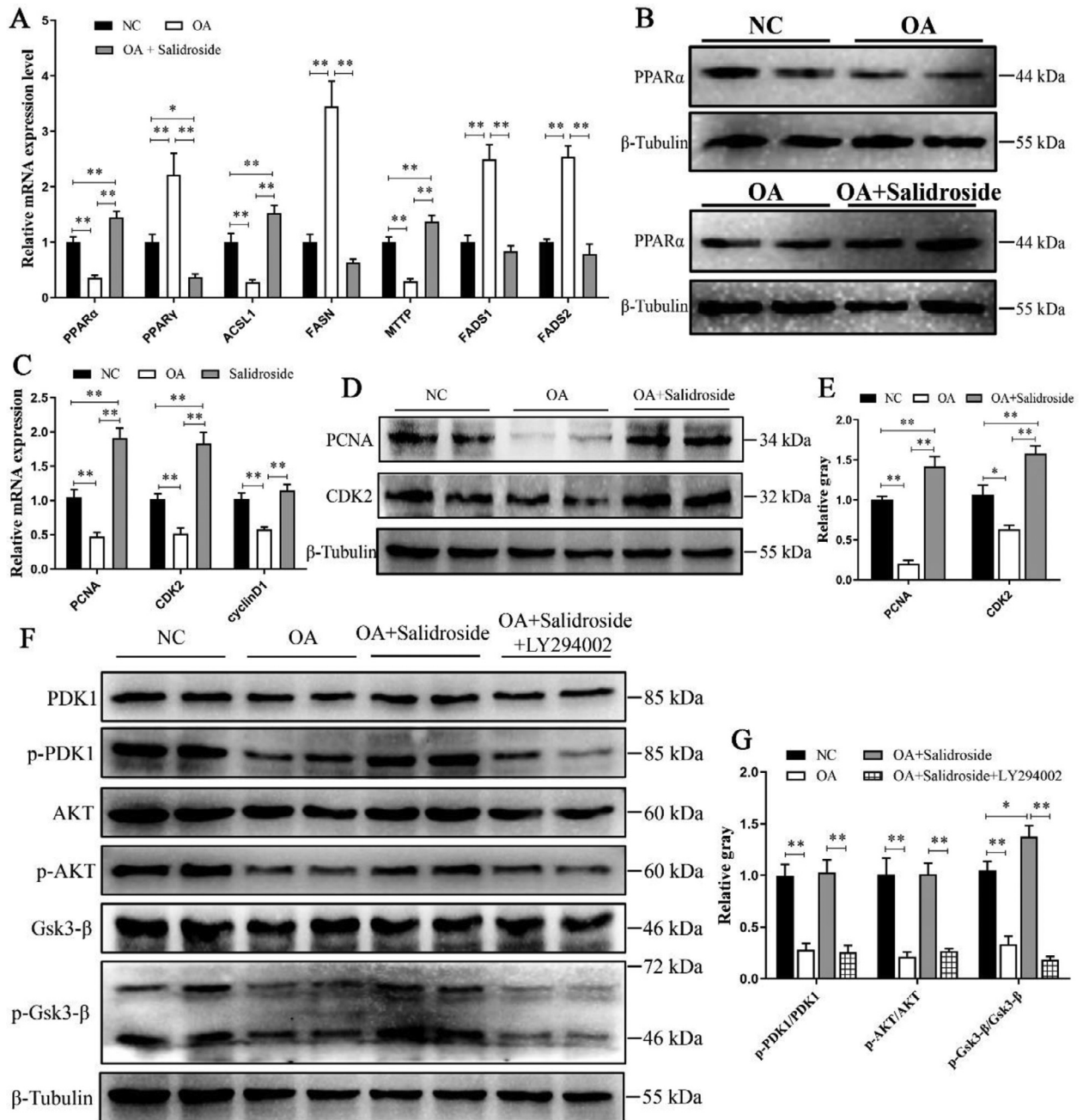
Figure 3. SDS inhibits OA-induced lipid accumulation and promotes proliferation via PI3K/AKT/Gsk3-β pathway in chicken primary hepatocytes. (A) The mRNA expression abundances of lipid metabolism related genes. (B) The protein level of PPARα was detected by western blot. (C) The mRNA expression of proliferation related genes. (D, E) The protein expression of PCNA and CDK2 were detected by western blot. (F, G) The total protein and phosphorylation levels of PDK1, AKT, and Gsk3-β were detected by western blot. Abbreviations: NC, negative control; OA: oleic acid; PPARα/γ, peroxisome proliferator-activated receptor-alpha/gamma. LY294002: PI3K inhibitor. Replications = 3. Bars represent SEM; *$P <$ 0.05 and **$P <$ 0.01.

red O staining showed that numerous lipid droplets appeared in the liver, which indicated severe steatosis. In group Con + SDS and Model + SDS, we observed that the hepatocytes were arranged neatly and clearly, the nucleus were at the center of the cell (blue) and the cytoplasm of the hepatocytes were evenly distributed (pink). Oil red O staining showed that both Con + SDS and Model + SDS groups had fewer fat droplets than the Con group (Figure 5).

Compared with the Con group, both TC and TG levels in serum were significantly increased in the Model group, as well as decreased in the Con + SDS and

Model + SDS groups ($P <$ 0.05). The ALT and AST levels in group Con + SDS and Model + SDS were significantly lower than those in Model group ($P <$ 0.05). Moreover, we found that SOD activity in group Con + SDS was higher than those in group Con and Model ($P <$ 0.05, Table 7).

Compared with the Con group, the mRNA expression abundances of *PPARα* and *MTTP* was significantly increased in the group Con + SDS and Model + SDS ($P <$ 0.05). The mRNA expressions abundances of *PPARγ, SCD*, and *FAS* were significantly increased in the Model group, whereas they
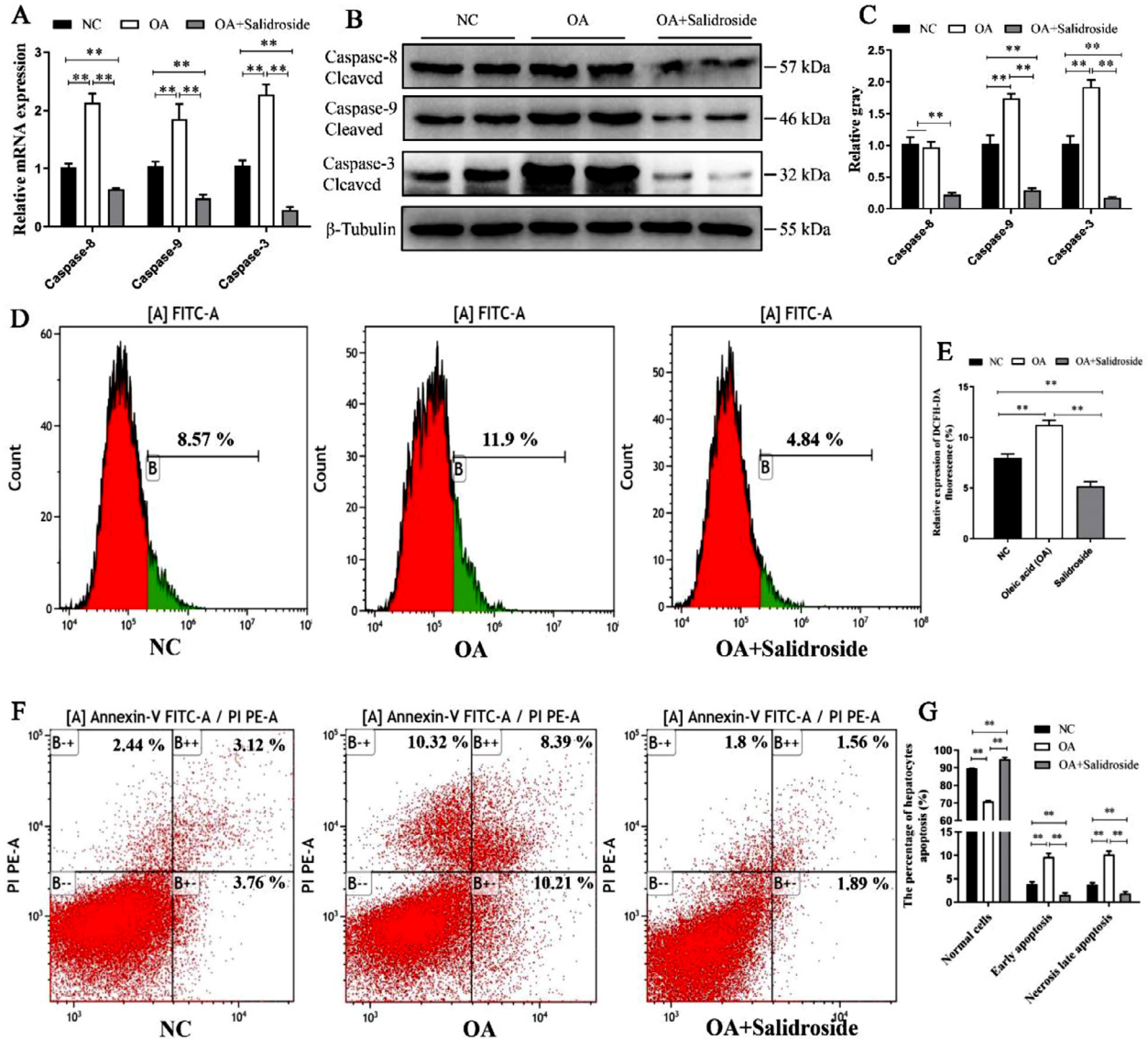
Figure 4. SDS inhibits hepatocyte apoptosis in an OA-induced fatty liver model. (A) The mRNA expression of apoptosis related genes (Caspase-8, Caspase-9, and Caspase-3). (B, C) Western blot analysis revealed the levels of Caspase-8, Caspase-9, and Caspase-3 cleavage. (D, E) ROS levels in chicken primary hepatocytes were determined by FITC-staining flow cytometry with an excitation wavelength of 488 nm and an emission wavelength of 525 nm. (F, G) Apoptotic hepatocytes were detected by annexin V-FITC/PI-staining flow cytometry. Abbreviations: NC, negative control; OA, oleic acid; ROS, reactive oxygen species. Replications = 3. Bars represent SEM; $*P < 0.05$ and $**P < 0.01$.

were decreased in the Con + SDS and Model + SDS group ($P < 0.05$). Moreover, the mRNA expressions of *TNF-α, IL-1β, IL-6,* and *IL-8* were significantly increased in the Model group while decreased in the Con + SDS and Model + SDS groups ($P < 0.05$; Table 8). Our results suggest that SDS alleviates high-fat diet-induced hepatic steatosis, oxidative stress and the inflammatory response of laying hens in vivo.

DISCUSSION

Fatty liver hemorrhagic syndrome is a chronic hepatic disease caused by a disorder of lipid metabolism, which usually presents as steatosis, cirrhosis, liver fibrosis, and NAFLD (McCullough, 2004; Cheng et al., 2018). FLHS occurs in cage laying hens with high frequency and is characterized by decreased egg production and unexplained death of laying hens. FLHS accounts for 74% of

Table 4. Effects of SDS feeding on the levels of biochemical parameters in the serum.

Biochemical parameters	Control	5 mg/kg	10 mg/kg	20 mg/kg	40 mg/kg	80 mg/kg
TC (mmol/L)	17.36±2.28 [a]	16.08±2.18 [ab]	9.8±1.89 [cd]	4.74±1.19 [d]	8.04±2.37 [cd]	10.85±1.69 [bc]
TG (mmol/L)	26.93±3.46 [a]	27.78±3.92 [a]	18.76±3.14 [ab]	7.85±2.52 [c]	13.34±4.07 [bc]	18.22±3.37 [abc]
ALT (U/L)	9.81±1.12 [b]	14.06±1.14 [a]	4.15±1.55 [cd]	3.72±0.56 [d]	5.64±0.92 [cd]	7.08±0.58 [bc]
AST (U/L)	1214.36±121.67 [a]	60.52±9.24 [b]	78.74±9.8 [b]	41.91±8.24 [b]	56.28±5.14 [b]	47.55±3.06 [b]
SOD (U/mL)	22.46±1.41 [a]	17.92±2.41 [b]	23.09±0.65 [a]	24.1±0.78 [a]	21.99±1.32 [ab]	25.17±1.38 [a]

Abbreviations: ALT, alanine aminotransferase; AST, aspartate aminotransferase; SOD, superoxide dismutase; TC, total cholesterol; TG, triglyceride. Data was shown as the mean ± standard error (SE) (n = 9).
[a,b,c,d]Means in the same row marked without a common superscript letter differed significantly ($P < 0.05$).

Table 5. Effects of SDS feeding on the mRNA expression of lipid metabolism related genes and proinflammatory cytokines in chicken liver.

Genes	Control	5 mg/kg	10 mg/kg	20 mg/kg	40 mg/kg	80 mg/kg
PPARα	1.02±0.06 [c]	1.79±0.13 [bc]	1.83±0.19 [bc]	2.26±0.20 [a]	2.12±0.52 [a]	1.78±0.26 [bc]
PPARγ	1.01±0.20 [b]	1.24±0.12 [ab]	1.15±0.23 [ab]	1.63±0.28 [a]	0.33±0.07 [c]	0.34±0.03 [c]
MTTP	1.02±0.15 [c]	3.29±0.65 [ab]	2.73±0.45 [abc]	4.00±0.89 [a]	2.06±0.23 [bc]	1.70±0.19 [bc]
FASN	0.99±0.11 [a]	0.35±0.04 [b]	0.79±0.08 [a]	0.42±0.03 [b]	0.31±0.11 [b]	0.46±0.12 [b]
IL-6	1.01±0.13 [a]	0.6±0.07 [bc]	0.74±0.06 [b]	0.37±0.11 [c]	0.54±0.04 [bc]	0.54±0.1 [bc]
IL-1β	1.01±0.07 [a]	1.00±0.09 [a]	0.38±0.03 [bc]	0.57±0.1 [b]	0.33±0.07 [c]	0.43±0.05 [bc]

Abbreviations: FASN, fatty acid synthase; IL-6/1β, interleukin 6/1 beta; MTTP, microsomal triglyceride transport protein; PPARα/γ, peroxisome proliferator-activated receptor-alpha/gamma. Data was shown as the mean ± standard error (SE) (n = 9).
[a,b,c]Means in the same row marked without a common superscript letter differed significantly ($P < 0.05$).

Table 6. Body, liver, and abdominal fat weight measurements.

Weight (g)	Con	Con + SDS	Model	Model + SDS
Body (0 d)	1,760±190	1,740±190	1,730±140	1,740±130
Body (28 d)	1,770±110 [b]	1,650±110 [c]	1,920±150 [a]	1,700±90 [c]
Liver	50.67±7.52 [b]	33.53±3.62 [c]	58.72±6.88 [a]	26.17±1.82 [c]
Abdominal fat	72.34±15.35 [b]	33.05±12.52 [c]	94.98±16.12 [a]	40.97±13.02 [c]

Data was shown as the mean ± standard error (SE) (n = 9).
[a,b,c]Means within a row marked without the same superscripts differed significantly ($P < 0.05$).
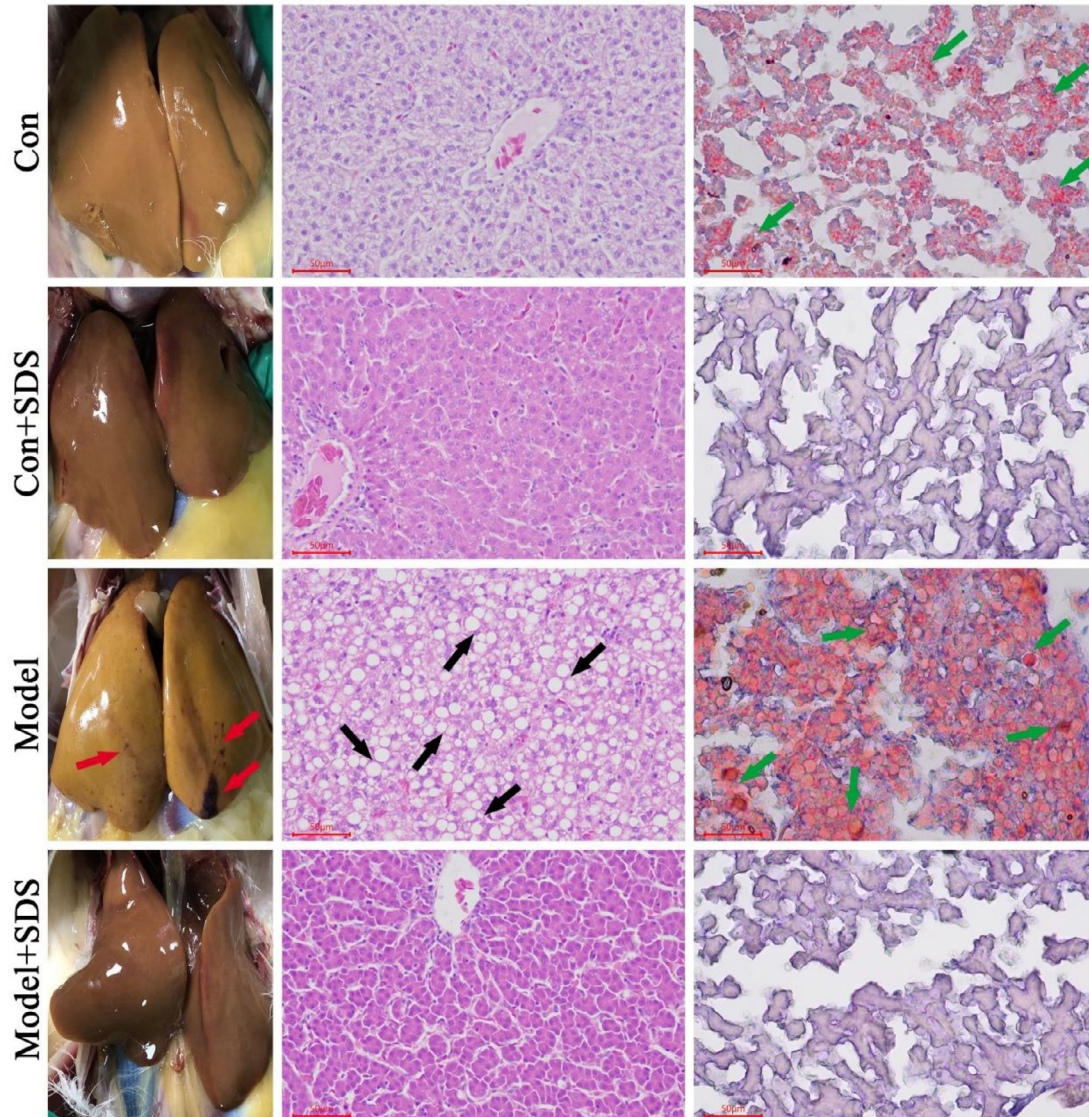

Figure 5. The morphological and histological characteristics of chicken liver. Hematoxylin-eosin (HE) staining and Oil red O staining were magnified 200 × . The black arrow indicates the "fatty vacuoles", the green arrow indicates the "lipid droplets", and the red arrow indicates severe pathological changes of the fatty liver-hemorrhagic syndrome of laying hens.

Table 7. Serum biochemical parameters were measured with ELISA kits.

Biochemical parameters	Con	Con + SDS	Model	Model + SDS
TC (mmol/L)	6.12±0.3 [b]	3.68±0.18 [c]	12.49±1.43 [a]	4.03±0.11 [bc]
TG (mmol/L)	15.65±0.7 [b]	11.31±0.27 [c]	23.25±0.59 [a]	11.48±0.62 [c]
ALT (U/L)	100.1±9.05 [a]	63.06±11.05 [b]	119.24±14.41 [a]	65.64±8.28 [b]
AST (U/L)	35.26±4.01 [b]	10.82±1.59 [c]	102.3±9.22 [a]	14.03±1.32 [c]
GSH (mgGSH/L)	10.82±1.15 [a]	7.12±0.51 [b]	13.4±1.87 [a]	5.86±0.49 [b]
SOD (U/mL)	119.66±4.12 [bc]	149.78±7.43 [a]	107.72±7.63 [c]	130.57±4.14 [b]

Abbreviations: ALT, alanine aminotransferase; AST, aspartate aminotransferase; GSH, glutathione; SOD, superoxide dismutase; TC, total cholesterol; TG, triglyceride. Data was shown as the mean ± standard error (SE) (n = 9).
[a,b,c]Means within a row marked without the same superscripts differed significantly ($P < 0.05$).

the total mortality of cage laying hens in Queensland, Australia (Rozenboim et al., 2016). In addition, FLHS is the most common cause of non-communicable chicken deaths in Northern California (Mete et al., 2013). FLHS caused huge losses to the poultry industry.

RRL is a herbal drug which grows at high altitude areas (Booker et al., 2016) and SDS has numerous pharmacological effects, such as protective effects on mitochondrial function (Zhang et al., 2015), antiapoptotic and anti-inflammatory effects (Zhu et al., 2015), and antioxidant effects (Li et al., 2012; Xiao et al., 2014). Multiple studies suggested that SDS could reduce the liver lipid accumulation in both the type 2 diabetic (Zhang et al., 2016b) and NAFLD mice (Zheng et al., 2018). In the current study, we found that SDS inhibited OA-induced lipid accumulation in primary chicken hepatocytes. Moreover, SDS promoted hepatocyte proliferation and inhibited its apoptosis in an OA-induced fatty liver model. SDS increased the hepatocyte activity and the mRNA expression of proliferation related genes *PCNA, CDK2,* and *cyclinD1*, and the protein expression levels of PCNA and CDK2. Moreover, SDS decreased the cleavage levels of Caspase-9, Caspase-8, and Caspase-3, and also the hepatocytes apoptosis. These results were consistent with the previous studies which indicated that SDS increased the protein expression of cyclin-dependent kinases (**CDKs**) (Mao et al., 2015) and Cyclin D1 (Tian et al., 2018), and suppressed cell apoptosis by inhibiting the proapoptotic protein expression of cleaved-Caspase-3/9 (Tian et al., 2018). Our

study showed that SDS significantly attenuated OA-induced ROS generation, which was consistent with the finding that SDS attenuated high-fat diet-induced ROS generation in NAFLD mice (Zheng et al., 2018).

PI3K/AKT/Gsk3-β is a critical antiapoptotic signaling pathway which activates a series of growth signaling pathways and blocks apoptotic signaling pathways, thereby promoting cell survival and proliferation (Pap and Cooper, 1998; Zhang et al., 2016a). Zhang et al. suggested that SDS protected against 1-methyl-4-phenylpyridine-induced cell apoptosis in part by regulating the PI3K/AKT/Gsk3-β pathway. SDS increased the phosphorylation levels of AKT and Gsk3-β, and inhibited the activation of caspase-3, caspase-6, and caspase-9 (Zhang et al., 2016a). SDS dose-dependently increased the phosphorylation of the mitochondria-associated PI3K/AKT/Gsk3-β pathway in hepatocytes (Zheng et al., 2015), and alleviated sepsis induced myocarditis in rats by regulating the PI3K/AKT/Gsk3-β signaling pathway (He et al., 2015). In the present study, we found that SDS increased the phosphorylation levels of PDK1, AKT, and Gsk3-β but decreased the PI3K inhibitor. We determined that SDS alleviated lipid accumulation, hepatocyte apoptosis, and promoted hepatocyte proliferation in the OA-induced fatty liver model by targeting the PI3K/AKT/Gsk3-β pathway.

Furthermore, we investigated the effects of SDS on HFD-induced FLHS in laying hens *in vivo*. We found that SDS dose-dependently decreased TC, TG, ALT, and AST levels in the serum, inhibited lipid accumulation and the expression abundance of inflammatory factors in the liver. These results indicated that the layer's body weight, liver weight, and abdominal fat weight were significantly increased in the Model group with severe steatosis, whereas all those traits were decreased and improved in SDS feeding groups. Additionally, high-fat diet-induced FLHS of laying hens showed the high levels of TC, TG, ALT, and AST in serum, while SDS improved all those indexes and increased SOD activity of high-fat diet-fed birds. Zheng et al. detected that SDS dose-dependently alleviated hepatic steatosis, oxidative stress, and inflammatory reactions in the liver of NAFLD mice, characterized by the decreased levels of TC, TG, ALT, and AST in serum, inhibition of hepatic lipid deposition and the gene expression of FAS, and suppression of the gene expression of *TNF-α* and *IL-1β* in the liver (Zheng et al., 2018). Moreover, SDS

Table 8. SDS alleviates high-fat diet-induced hepatic steatosis and inflammatory response of laying hens in vivo.

Genes	Con	Con + SDS	Model	Model + SDS
PPARα	1.02±0.08 [b]	2.16±0.12 [a]	0.74±0.15 [b]	2.13±0.48 [a]
PPARγ	1.02±0.13 [b]	0.26±0.07 [c]	1.61±0.05 [a]	0.25±0.05 [c]
FASN	1.00±0.07 [b]	0.37±0.05 [c]	1.53±0.16 [a]	0.47±0.06 [c]
SCD	0.99±0.03 [b]	0.21±0.08 [c]	2.14±0.27 [a]	0.47±0.09 [c]
MTTP	0.99±0.12 [b]	2.91±0.4 [a]	0.20±0.02 [b]	2.04±0.31 [a]
TNF-*α*	1.01±0.16 [b]	0.35±0.04 [c]	1.89±0.35 [a]	0.39±0.04 [c]
IL-1β	0.99±0.04 [b]	0.29±0.06 [d]	1.78±0.18 [a]	0.60±0.07 [c]
IL-6	1.00±0.09 [b]	0.47±0.05 [c]	2.61±0.23 [a]	0.56±0.09 [c]
IL-8	1.02±0.06 [b]	0.61±0.09 [c]	1.87±0.19 [a]	0.74±0.04 [bc]

Abbreviations: FASN, fatty acid synthase; IL-1β/6/8, interleukin-1 beta/6/8; MTTP, microsomal triglyceride transport protein; PPARα/γ, peroxisome proliferator-activated receptor-alpha/gamma; SCD, stearoyl-CoA desaturase; TNF-α, tumor necrosis factor alpha. Data was shown as the mean ± standard error (SE) (n = 9).
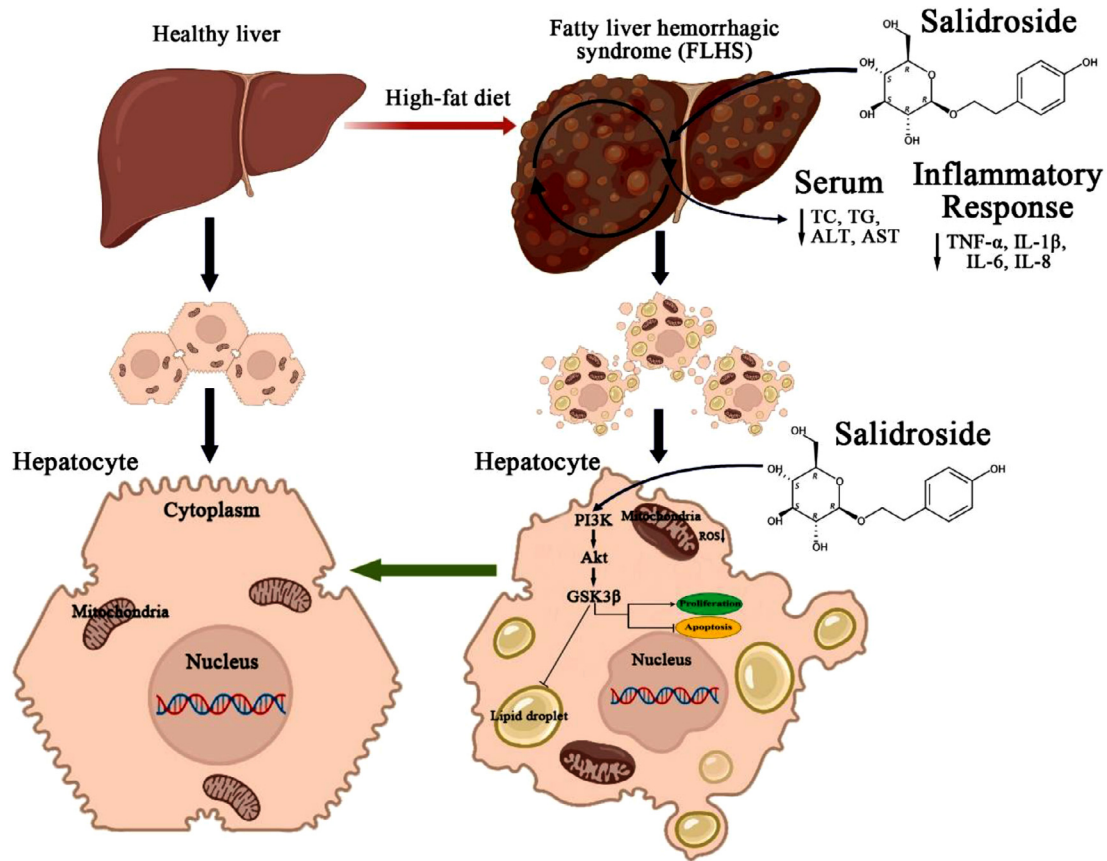[a,b,c]Means within a row marked without the same superscripts differed significantly ($P < 0.05$).

Figure 6. A summary of the regulatory mechanisms of SDS in an oleic acid (OA)-induced fatty liver model and a high-fat diet-induced FLHS of laying hens in vitro and in vivo.

dose-dependently regulated lipid accumulation and ROS generation in cultured hepatocytes to alleviate high-fat-diet-induced nonalcoholic fatty liver disease (Zheng et al., 2018), decreased inflammasome axis such as Caspase-1 and IL-1β and improved the increased levels of serum TC and TG in diabetic rats (Zheng et al., 2021), as well as improve lipid profiles in the serum and liver through activation of mitochondria-related AMPK/PI3K/Akt/GSK3β pathway (Zheng et al., 2015). Amevor et al. (2021) reported a decreased levels of AST and ALT in the serum, and also observed no liver steatosis in chickens fed with the diets containing both dietary quercetin and vitamin E (dietary antioxidants). The increased expression of lipogenesis gene FAS accelerated the ectopic deposition of TG (Foretz et al., 1998). In the current study, we found that SDS decreased the liver mRNA expression of *PPARγ, SCD,* and *FAS,* whereas increased the mRNA expression of *PPARα* and *MTTP* in high-fat diet-induced FLHS of laying hens in vivo. Inflammatory cytokine such as TNF-α, IL-6, IL-8, and IL-1β played important roles in the inflammatory response (Jain et al., 2009). Previous studies reported that SDS alleviated cell injury and lipid accumulation, and inhibited the mRNA expression of *IL-1β* and *IL-6* in human NAFLD (Feng et al., 2019), alleviated LPS-induced injury in humans by decreasing inflammatory chemokines IL-6 and TNF-α (Tian et al., 2018), and improved the survival rate of endotoxemia mice by blocking the activation of NF-κB and inhibiting the expression and release of inflammatory cytokines TNF-α, IL-6, and IL-1β (Guan et al., 2011). We found that SDS decreased the mRNA expression of *TNF-α, IL-1β, IL-6,* and *IL-8.* These results indicate that SDS alleviates HFD-induced hepatic steatosis, oxidative stress, and the inflammatory response of laying hens in vivo.

CONCLUSIONS

In the present study, we investigated the effects of SDS on FLHS by establishing Oleic acid (OA)-induced fatty liver model and high-fat diet-induced FLHS in vitro and in vivo, respectively. We observed that SDS attenuated ROS generation, inhibited lipid accumulation and hepatocyte apoptosis, and promoted hepatocyte proliferation in the OA-induced fatty liver model in vitro by targeting the PI3K/AKT/Gsk3-β pathway. Moreover, SDS alleviated high-fat-diet-induced hepatic steatosis, oxidative stress, and the inflammatory response of the laying hens in vivo (Figure 6).

ACKNOWLEDGMENTS

DISCLOSURES

The authors have declared that no competing interest exists.

REFERENCES

Amevor, F. K., Z. Cui, X. Du, Z. Ning, G. Shu, N. Jin, X. Deng, Y. Tian, Z. Zhang, X. Kang, D. Xu, G. You, Y. Zhang, D. Li, Y. Wang, Q. Zhu, and X. Zhao. 2021. Combination of quercetin and vitamin E supplementation promotes yolk precursor synthesis and follicle development in aging breeder hens via liver−blood−ovary signal axis. Animals 11:1915.

Booker, A., B. Jalil, D. Frommenwiler, E. Reich, L. Zhai, Z. Kulic, and M. Heinrich. 2016. The authenticity and quality of Rhodiola rosea products. Phytomedicine 23:754–762.

Butler, E. J. 1976. Fatty liver diseases in the domestic fowl−a review. Avian pathol. 5:1–14.

Cheng, S., S. Liang, Q. Liu, Z. Deng, Y. Zhang, J. Du, Y. Zhang, S. Li, B. Cheng, and C. Ling. 2018. Diosgenin prevents high-fat diet-induced rat non-alcoholic fatty liver disease through the AMPK and LXR signaling pathways. Int. J. Mol. Med. 41:1089–1095.

Cui, Z., F. K. Amevor, Q. Feng, X. Kang, W. Song, Q. Zhu, Y. Wang, D. Li, and X. Zhao. 2020a. Sexual maturity promotes yolk precursor synthesis and follicle development in hens via liver-blood-ovary signal axis. Animals (Basel) 10:2348.

Cui, Z., L. Liu, F. Kwame Amevor, Q. Zhu, Y. Wang, D. Li, G. Shu, Y. Tian, and X. Zhao. 2020b. High expression of miR-204 in chicken atrophic ovaries promotes granulosa cell apoptosis and inhibits autophagy. Front. Cell Dev. Biol. 8:580072.

Cui, Z., X. Shen, X. Zhang, F. Li, F. K. Amevor, Q. Zhu, Y. Wang, D. Li, G. Shu, Y. Tian, and X. Zhao. 2021. A functional polymorphism of inhibin alpha subunit at miR-181b-1-3p-binding site regulates proliferation and apoptosis of chicken ovarian granular cells. Cell Tissue Res. 384:545–560.

Dhar, P., P. K. Bajpai, A. B. Tayade, O. P. Chaurasia, R. B. Srivastava, and S. B. Singh. 2013. Chemical composition and antioxidant capacities of phytococktail extracts from trans-Himalayan cold desert. BMC Complem. Altern. M. 13:259.

Egnatchik, R. A., A. K. Leamy, Y. Noguchi, M. Shiota, and J. D. Young. 2014. Palmitate-induced activation of mitochondrial metabolism promotes oxidative stress and apoptosis in H4IIEC3 rat hepatocytes. Metabolism 63:283–295.

Espe, M., S. Xie, P. Araujo, and E. Holen. 2019. Development of a fatty liver model using oleic acid in primary liver cells isolated from Atlantic salmon and the prevention of lipid accumulation using metformin. Aquacult. Nutr. 25:737–746.

Feng, J., P. Niu, K. Chen, L. Wu, T. Liu, S. Xu, J. Li, S. Li, W. Wang, X. Lu, Q. Yu, N. Liu, L. Xu, F. Wang, W. Dai, Y. Xia, X. Fan, and C. Guo. 2018. Salidroside mediates apoptosis and autophagy inhibition in concanavalin A-induced liver injury. Exp. Ther. Med. 15:4599–4614.

Feng, Q., C. Liu, W. Gao, X. L. Geng, and N. Dai. 2019. Salidroside-mitigated inflammatory injury of hepatocytes with non-alcoholic fatty liver disease via inhibition TRPM2 ion channel activation. Diabetes Metab. Syndr. Obes. 12:2755–2763.

Feng, X., W. Yu, X. Li, F. Zhou, W. Zhang, Q. Shen, J. Li, C. Zhang, and P. Shen. 2017. Apigenin, a modulator of PPARγ, attenuates HFD-induced NAFLD by regulating hepatocyte lipid metabolism

and oxidative stress via Nrf2 activation. Biochem. Pharmacol. 136:136–149.

Foretz, M., D. Carling, C. Guichard, P. Ferré, and F. Foufelle. 1998. AMP-activated protein kinase inhibits the glucose-activated expression of fatty acid synthase gene in rat hepatocytes. J. Biol. Chem. 273:14767–14771.

Guan, S., H. Feng, B. Song, W. Guo, Y. Xiong, G. Huang, W. Zhong, M. Huo, N. Chen, J. Lu, and X. Deng. 2011. Salidroside attenuates LPS-induced pro-inflammatory cytokine responses and improves survival in murine endotoxemia. Int. Immunopharmacol. 11:2194–2199.

Guan, S., Y. Xiong, B. Song, Y. Song, D. Wang, X. Chu, N. Chen, M. Huo, X. Deng, and J. Lu. 2012. Protective effects of salidroside from Rhodiola rosea on LPS-induced acute lung injury in mice. Immunopharm. Immunot. 34:667–672.

He, H., X. Chang, J. Gao, L. Zhu, M. Miao, and T. Yan. 2015. Salidroside mitigates sepsis-induced myocarditis in rats by regulating IGF-1/PI3K/Akt/GSK-3β signaling. Inflammation 38:2178–2184.

Huang, W. C., Y. L. Chen, H. C. Liu, S. J. Wu, and C. J. Liou. 2018. Ginkgolide C reduced oleic acid-induced lipid accumulation in HepG2 cells. Saudi. Pharm. J. 26:1178–1184.

Jain, S. K., J. Rains, J. Croad, B. Larson, and K. Jones. 2009. Curcumin supplementation lowers TNF-alpha, IL-6, IL-8, and MCP-1 secretion in high glucose-treated cultured monocytes and blood levels of TNF-alpha, IL-6, MCP-1, glucose, and glycosylated hemoglobin in diabetic rats. Antioxid. Redox Signal. 11:241–249.

Jensen, L. S., J. M. Casey, S. I. Savage, and W. M. Britton. 1976. An association of hardness of water with incidence of fatty liver syndrome in laying hens. Poult. Sci. 55:719–724.

Koek, G. H., P. R. Liedorp, and A. Bast. 2011. The role of oxidative stress in non-alcoholic steatohepatitis. Clin. Chim. Acta. 412: 1297–1305.

Koo, S. H. 2013. Nonalcoholic fatty liver disease: molecular mechanisms for the hepatic steatosis. Clin. Mol. Hepatol. 19:210–215.

Li, D., Y. Fu, W. Zhang, G. Su, B. Liu, M. Guo, F. Li, D. Liang, Z. Liu, X. Zhang, Y. Cao, N. Zhang, and Z. Yang. 2013. Salidroside attenuates inflammatory responses by suppressing nuclear factor-κB and mitogen activated protein kinases activation in lipopolysaccharide-induced mastitis in mice. Inflamm. Res. 62:9–15.

Li, F., H. Tang, F. Xiao, J. Gong, Y. Peng, and X. Meng. 2011. Protective effect of salidroside from Rhodiolae Radix on diabetes-induced oxidative stress in mice. Molecules (Basel, Switzerland) 16:9912–9924.

Li, L., X. Chu, Y. Yao, J. Cao, Q. Li, and H. Ma. 2020. (-)-Hydroxycitric acid alleviates oleic acid-induced steatosis, oxidative stress, and inflammation in primary chicken hepatocytes by regulating AMP-activated protein kinase-mediated reactive oxygen species levels. J. Agric. Food Chem. 68:11229–11241.

Li, X., J. Sipple, Q. Pang, and W. Du. 2012. Salidroside stimulates DNA repair enzyme Parp-1 activity in mouse HSC maintenance. Blood 119:4162–4173.

Lin, S. Y., X. Dan, X. X. Du, C. L. Ran, X. Lu, S. J. Ren, Z. T. Tang, L. Z. Yin, C. L. He, Z. X. Yuan, H. L. Fu, X. L. Zhao, and G. Shu. 2019. Protective effects of salidroside against carbon tetrachloride (CCl(4))-induced liver injury by initiating mitochondria to resist oxidative stress in mice. Int. J. Mol. Sci. 20:3187.

Liu, G. Y., Y. Z. Sun, N. Zhou, X. M. Du, J. Yang, and S. J. Guo. 2016. 3,3′-OH curcumin causes apoptosis in HepG2 cells through ROS-mediated pathway. Eur. J. Med. Chem. 112:157–163.

Livak, K. J., and T. D. Schmittgen. 2001. Analysis of relative gene expression data using real-time quantitative PCR and the 2(-Delta Delta C(T)) Method. Methods (San Diego, Calif.) 25:402–408.

Lu, L., J. Yuan, and S. Zhang. 2013. Rejuvenating activity of salidroside (SDS): dietary intake of SDS enhances the immune response of aged rats. Age (Dordrecht, Netherlands) 35:637–646.

Lv, C., Y. Huang, Z. X. Liu, D. Yu, and Z. M. Bai. 2016. Salidroside reduces renal cell carcinoma proliferation by inhibiting JAK2/STAT3 signaling. Cancer Biomark. 17:41–47.

Mantena, S. K., A. L. King, K. K. Andringa, H. B. Eccleston, and S. M. Bailey. 2008. Mitochondrial dysfunction and oxidative stress in the pathogenesis of alcohol- and obesity-induced fatty liver diseases. Free Radic. Biol. Med. 44:1259–1272.

Mao, G. X., H. B. Deng, L. G. Yuan, D. D. Li, Y. Y. Li, and Z. Wang. 2010. Protective role of salidroside against aging in a

mouse model induced by D-galactose. Biomed. Environ. Sci. 23:161–166.

Mao, G. X., W. M. Xing, X. L. Wen, B. B. Jia, Z. X. Yang, Y. Z. Wang, X. Q. Jin, G. F. Wang, and J. Yan. 2015. Salidroside protects against premature senescence induced by ultraviolet B irradiation in human dermal fibroblasts. Int. J. Cosmet. Sci. 37:321–328.

Maurice, D. V., and L. S. Jensen. 1978. Influence of diet composition on hepatic lipid accumulation and hemorrhages in caged layers. Poult. Sci. 57:989–997.

McCullough, A. J. 2004. The clinical features, diagnosis and natural history of nonalcoholic fatty liver disease. Clin. Liver Dis. 8:521–533 viii.

Mete, A., F. Giannitti, B. Barr, L. Woods, and M. Anderson. 2013. Causes of mortality in backyard chickens in northern California: 2007-2011. Avian Diseases. 57:311–315.

Neuschwander-Tetri, B. A. 2007. Fatty liver and the metabolic syndrome. Curr. Opin. Gastroenterol. 23:193–198.

Pap, M., and G. M. Cooper. 1998. Role of glycogen synthase kinase-3 in the phosphatidylinositol 3-Kinase/Akt cell survival pathway. J. Biol. Chem. 273:19929–19932.

Prieto, I., and M. Monsalve. 2017. ROS homeostasis, a key determinant in liver ischemic-preconditioning. Redox Biol. 12:1020–1025.

Qi, X. L., J. Wang, H. Y. Yue, S. G. Wu, Y. N. Zhang, H. M. Ni, Y. Guo, H. J. Zhang, and G. H. Qi. 2018. Trans10, cis12-conjugated linoleic acid exhibits a stronger antioxidant capacity than cis9, trans11-conjugated linoleic acid in primary cultures of laying hen hepatocytes. Poult. Sci. 97:4415–4424.

Reccia, I., J. Kumar, C. Akladios, F. Virdis, M. Pai, N. Habib, and D. Spalding. 2017. Non-alcoholic fatty liver disease: a sign of systemic disease. Metabolism 72:94–108.

Rozenboim, I., J. Mahato, N. A. Cohen, and O. Tirosh. 2016. Low protein and high-energy diet: a possible natural cause of fatty liver hemorrhagic syndrome in caged White Leghorn laying hens. Poult. Sci. 95:612–621.

Shini, A., S. Shini, and W. L. Bryden. 2019. Fatty liver haemorrhagic syndrome occurrence in laying hens: impact of production system. Avian Pathol. 48:25–34.

Squires, E. J., and S. Leeson. 1988. Aetiology of fatty liver syndrome in laying hens. Br. Vet. J. 144:602–609.

Tian, F., Z. Chen, Y. Zhang, J. Jiang, and T. Li. 2018. Salidroside protects LPS-induced injury in human thyroid follicular epithelial cells by upregulation of MiR-27a. Life Sci. 213:1–8.

Wang, L. J., H. W. Zhang, J. Y. Zhou, J. Liu, Y. Yang, X. L. Chen, C. H. Zhu, R. D. Zheng, W. H. Ling, and H. L. Zhu. 2014. Betaine attenuates hepatic steatosis by reducing methylation of the MTTP promoter and elevating genomic methylation in mice fed a high-fat diet. J. Nutr. Biochem. 25:329–336.

Wang, X., C. Xing, F. Yang, S. Zhou, G. Li, C. Zhang, H. Cao, and G. Hu. 2020. Abnormal expression of liver autophagy and apoptosis-related mRNA in fatty liver haemorrhagic syndrome and improvement function of resveratrol in laying hens. Avian Pathol. 49:171–178.

Weijler, A. M., B. Schmidinger, S. Kapiotis, H. Laggner, and M. Hermann. 2018. Oleic acid induces the novel apolipoprotein O and reduces mitochondrial membrane potential in chicken and human hepatoma cells. Biochimie 147:136–142.

Wolford, J. H., and D. Polin. 1972. Lipid accumulation and hemorrhage in livers of laying chickens. A study on fatty liver-hemorrhagic syndrome (FLHS). Poult. Sci. 51:1707–1713.

Wu, Y. L., L. H. Lian, Y. Z. Jiang, and J. X. Nan. 2009. Hepatoprotective effects of salidroside on fulminant hepatic failure induced by D-galactosamine and lipopolysaccharide in mice. J. Pharm. Pharmacol. 61:1375–1382.

Wu, Y. L., D. M. Piao, X. H. Han, and J. X. Nan. 2008. Protective effects of salidroside against acetaminophen-induced toxicity in mice. Biol. Pharm. Bull. 31:1523–1529.

Xiao, L., H. Li, J. Zhang, F. Yang, A. Huang, J. Deng, M. Liang, F. Ma, M. Hu, and Z. Huang. 2014. Salidroside protects Caenorhabditis elegans neurons from polyglutamine-mediated toxicity by reducing oxidative stress. Molecules (Basel, Switzerland) 19:7757–7769.

Xiong, Y., Y. Wang, Y. Xiong, W. Gao, and L. Teng. 2020. Salidroside alleviated hypoxia-induced liver injury by inhibiting endoplasmic reticulum stress-mediated apoptosis via IRE1α/JNK pathway. Biochem. Biophys. Res. Commun. 529:335–340.

Yang, F., J. Ruan, T. Wang, J. Luo, H. Cao, Y. Song, J. Huang, and G. Hu. 2017. Improving effect of dietary soybean phospholipids supplement on hepatic and serum indexes relevant to fatty liver hemorrhagic syndrome in laying hens. Anim. Sci. J. 88:1860–1869.

Yang, Z. R., H. F. Wang, T. C. Zuo, L. L. Guan, and N. Dai. 2016. Salidroside alleviates oxidative stress in the liver with non- alcoholic steatohepatitis in rats. BMC Pharmacol. Toxicol. 17:16.

Yu, P., C. Hu, E. J. Meehan, and L. Chen. 2007. X-ray crystal structure and antioxidant activity of salidroside, a phenylethanoid glycoside. Chem. Biodivers. 4:508–513.

Yuan, Y., S. J. Wu, X. Liu, and L. L. Zhang. 2013. Antioxidant effect of salidroside and its protective effect against furan-induced hepatocyte damage in mice. Food Funct. 4:763–769.

Zhang, L., H. Yu, Y. Sun, X. Lin, B. Chen, C. Tan, G. Cao, and Z. Wang. 2007. Protective effects of salidroside on hydrogen peroxide-induced apoptosis in SH-SY5Y human neuroblastoma cells. Eur. J. Pharmacol. 564:18–25.

Zhang, W., H. He, H. Song, J. Zhao, T. Li, L. Wu, X. Zhang, and J. Chen. 2016a. Neuroprotective Effects of Salidroside in the MPTP Mouse Model of Parkinson's Disease: Involvement of the PI3K/Akt/GSK3β Pathway. Parkinson's Dis. 2016:9450137.

Zhang, W., M. Peng, Y. Yang, Z. Xiao, B. Song, and Z. Lin. 2015. Protective effects of salidroside on mitochondrial functions against exertional heat stroke-induced organ damage in the rat. Evid. Based Complement. Alternat. Med. 2015:504567.

Zhang, X. R., X. J. Fu, D. S. Zhu, C. Z. Zhang, S. Hou, M. Li, and X. H. Yang. 2016b. Salidroside-regulated lipid metabolism with down-regulation of miR-370 in type 2 diabetic mice. Eur. J. Pharmacol. 779:46–52.

Zheng, T., Q. Wang, F. Bian, Y. Zhao, W. Ma, Y. Zhang, W. Lu, P. Lei, L. Zhang, X. Hao, and L. Chen. 2021. Salidroside alleviates diabetic neuropathic pain through regulation of the AMPK-NLRP3 inflammasome axis. Toxicol. Appl. Pharmacol. 416:115468.

Zheng, T., X. Yang, W. Li, Q. Wang, L. Chen, D. Wu, F. Bian, S. Xing, and S. Jin. 2018. Salidroside attenuates high-fat diet-induced nonalcoholic fatty liver disease via AMPK-dependent TXNIP/NLRP3 pathway. Oxid. Med. Cell. Longev. 2018:8597897.

Zheng, T., X. Yang, D. Wu, S. Xing, F. Bian, W. Li, J. Chi, X. Bai, G. Wu, X. Chen, Y. Zhang, and S. Jin. 2015. Salidroside ameliorates insulin resistance through activation of a mitochondria-associated AMPK/PI3K/Akt/GSK3β pathway. Br. J. Pharmacol. 172:3284–3301.

Zhou, X. D., X. F. Dong, J. M. Tong, P. Xu, and Z. M. Wang. 2012. High levels of vitamin E affect retinol binding protein but not CYP26A1 in liver and hepatocytes from laying hens. Poult. Sci. 91:1135–1141.

Zhu, J., X. Wan, X. Zhu, X. Ma, Y. Zheng, and T. Zhang. 2010. Evaluation of salidroside in vitro and in vivo genotoxicity. Drug Chem. Toxicol. 33:220–226.

Zhu, L., T. Wei, J. Gao, X. Chang, H. He, F. Luo, R. Zhou, C. Ma, Y. Liu, and T. Yan. 2015. The cardioprotective effect of salidroside against myocardial ischemia reperfusion injury in rats by inhibiting apoptosis and inflammation. Apoptosis 20:1433–1443.

Zhuang, Y., C. Xing, H. Cao, C. Zhang, J. Luo, X. Guo, and G. Hu. 2019. Insulin resistance and metabonomics analysis of fatty liver haemorrhagic syndrome in laying hens induced by a high-energy low-protein diet. Sci. Rep. 9:10141.

Zuo, G., Z. Li, L. Chen, and X. Xu. 2007. Activity of compounds from Chinese herbal medicine Rhodiola kirilowii (Regel) Maxim against HCV NS3 serine protease. Antiviral Res. 76:86–92.